Development of Simplified Models for Solar Buildings Optimal Control

Michaël Kummert, Philippe André, Jacques Nicolas, Fondation Universitaire Luxembourgeoise, Avenue de Longwy, 185, B-6700 Arlon, Belgium
ph: +32/63/230859, fax: +32/63230800, E-mail: kummert@ful.ac.be

Introduction

The control operation is an essential feature of solar buildings, because of solar gains' random nature and intrinsic delay. Control systems must optimise passive and active gains, while preventing overheatings.
Our research's final objective is to apply modern control techniques such as optimal and adaptive predictive control to solar buildings. These techniques may be classified as model-based predictive methods and require a simplified model of the system to be controlled.
Most of the buildings control studies in the literature were made with very simple models, the emphasis being on original control algorithms [1 to 3]. Previous works have assessed the performance loss when those algorithms were used to control more realistic building models [4, 5]. They concluded to significant results deterioration, which lead to inefficient systems.
This work aims to develop a linear state-space thermal zone model suitable for our control applications, i.e. sufficiently accurate in the desired frequency range but not too complex for the control algorithms. Homogeneous slabs representations have been studied in order to obtain a thermal zone model suitable for control in [7, 8]. These works showed that second order slab models could give satisfactory results in this case. We study first, second and third order models for homogeneous and multilayer walls and their assembly into a zone model. This work is presented with more details in [0].

1. Wall modeling

Heat transfer through a one-dimensional slab (without sources) is governed by the heat diffusion equation, which can be expressed as:

$$\frac{\partial T(x,t)}{\partial t} = \alpha \frac{\partial^2 T(x,t)}{\partial x^2} \tag{1}$$

where α is the thermal diffusivity, supposed to be constant (for multilayer walls, this equation is solved separatly for each layer).
The boundary conditions are chosen as close as possible to the wall's situation in buildings: imposed air temperature (T_{a1} and T_{a2}) and radiative flux ϕ^r_1 and ϕ^r_2 on each side. They are different from the classical "equivalent quadripole" approach (see e.g. [9]), and were also used by Boileau et al. [7]. Their mathematical expression is:

$$k\frac{\partial T(x,t)}{\partial x}\bigg|_{x=0} = -\phi^r_1 - h_1\left(T_{a1} - T(0,t)\right) \qquad \text{and} \qquad k\frac{\partial T(x,t)}{\partial x}\bigg|_{x=e} = \phi^r_2 + h_2\left(T_{a2} - T(e,t)\right) \tag{2}$$

Initial conditions will always be in steady state at a uniform temperature of 0°C.
We studied step and frequency responses of both surface temperatures (T_{s1} and T_{s2}) to T_{a2} excitation only, because the dynamics of the response to ϕ^r_2 are identical (consider equation 2). Studied models are based on the electrical analogy and have one, two or three nodes per wall (see fig. 1). We modeled homogeneous slabs of three common materials (concrete, wood and insulation foam) and also multilayer:walls. These last ones were three heavy walls usually found in solar buildings: external wall (concrete-insulation foam-air-brick),:floor (light concrete-insulation material-reinforced concrete), roof (insulation material-air-tiles). The references used in our study were exact or high precision numerical solutions of the heat diffusion equation (1).

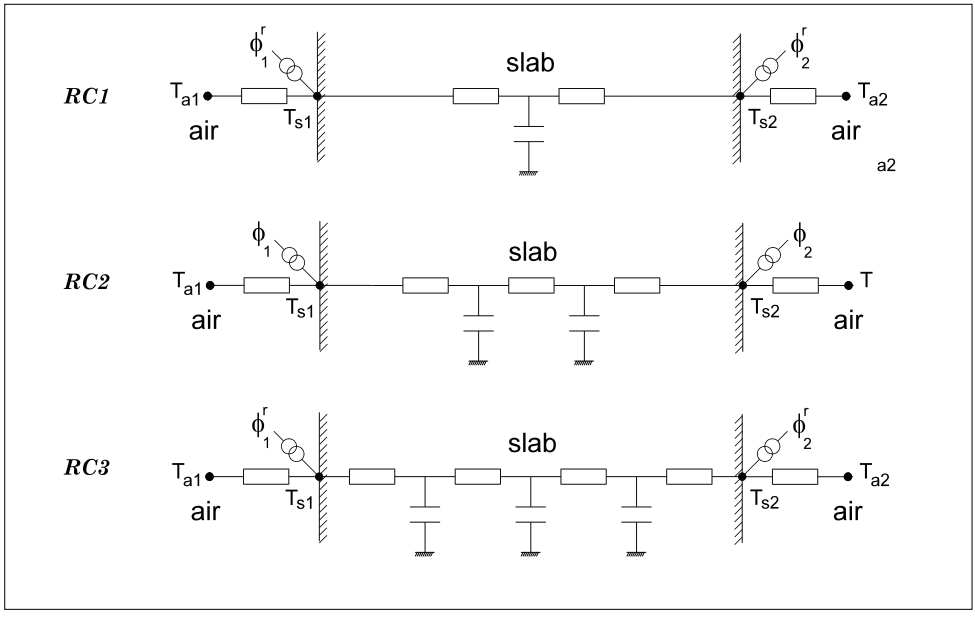

Figure 1: Studied wall models

We briefly sum up the obtained results here under (see [0] for more details).

Results

Step responses and Bode's curves show that a first order model (RC1) gives poor performances for all the modeled walls. The improvement obtained using the RC2 model is always very important, reducing for example the summed square error on step response to less than 10% of its initial value in every situation for the non-excited side. The RC3 model allows a far smaller additional improvement. The surface temperature responses on the excited side are always worse than those of the other side due to the absence of a thermal capacity between the excitation and the output (which causes an initial non-zero response). However, RC2 and RC3 responses are acceptable and we will see in section 2 that this inconvenient will be reduced by the wall incorporation in a zone model. In conclusion we see that, at this stage, the second order model seems to be the best compromise between accuracy and complexity.

2. Zone modeling

The thermal zone is the chosen base-unit for most of the building simulation programs. It represents a defined air volume at a uniform temperature and its definition is not unique. The zone's energy balance is given by:

$$C\frac{dT}{dt} = f(q_i)$$

where q_i are radiative and convective heat fluxes. The most complex contribution to this balance comes from the heat conduction through walls. Several methods can be applied to solve the heat conduction equation:

- z transform (discrete Laplace's transform), which is used in building simulation programs as the TYPE46 and TYPE56 multizone models of TRNSYS [6, 10].
- transmittance method, suitable for periodical evolution
- finite-difference method, that leads to "lumped capacitance" models if a small number of nodes is kept.

We used the "star network" obtained by assembling the wall models described in section 2,

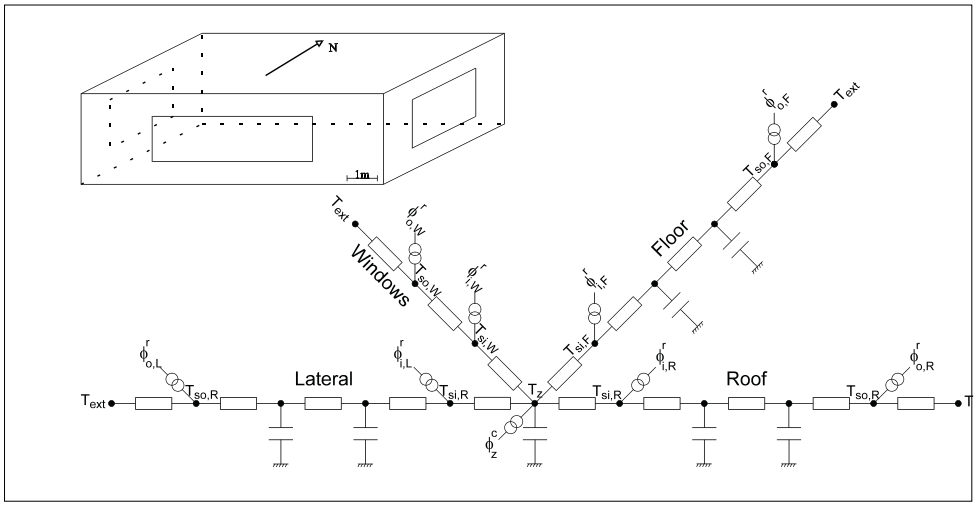

Figure 2 : example testcell and obtained RC2 model

which are connected to a central node representing the thermal capacity of the air volume inside the zone. This capacity is multiplied by 5 to account for convective transfers inside the zone [10]. Light walls (e.g. windows) are modeled by simple thermal resistances. Surface nodes without thermal capacity are kept, and receive radiative heat fluxes. The radiation distribution inside the zone is made according to area absorbtance weighted ratios. Radiative exchange between surfaces inside the zone is not considered explicitely, since we consider for the zone the resultant temperature, which globalise convective and radiative heat transfers. Both are linearised and included in the convective heat transfer coefficient between the wall and the zone. Convective heat fluxes (including natural convection, ventilation and infiltration) are directly introduced on the air node. Identical walls with the same boundary temperatures can be modeled together, summing areas and incoming radiations. This agglomeration can lead to a substantial model order reduction (e.g. in the case of identical lateral walls).

The chosen simulation example is a fictitious testcell presenting passive solar buildings characteristics (high thermal inertia, large windows, good insulation). The models are named after the number of nodes per wall, i.e. they keep the names RC1, RC2 and RC3. These names do not correspond to the total model order (respectively 4, 7 and 10). The fig. 2 represents the testcell and the obtained model with second order walls models (RC2). The TRNSYS TYPE 46, which has the same calculation engine as the belgian software MBDSA [10], will serve as a reference for our study.

Results

We studied the testcell step and frequency responses to 3 different excitations: external temperature, convective heating and solar radiation through windows. Afterwards, we simulated the zone using real meteorological data from a belgian Typical Meteorological Year (TMY). The table 1. gives a summary of the obtained errors for step responses. The good response obtained with RC2 and RC3 for an external temperature step is not

Table 1 : Testcell, sum of squared error for step responses

	convective heating		temperature		sunshine	
RC1	13.24	100.00 %	5.73	100.00 %	16.11	100.00 %
RC2	0.009	0.07 %	0.011	0.19 %	0.008	0.05 %
RC3	0.009	0.07 %	0.009	0.16 %	0.099	0.06 %

The zone temperature is reduced to [0,1] and the time is divided by the time constant

VI

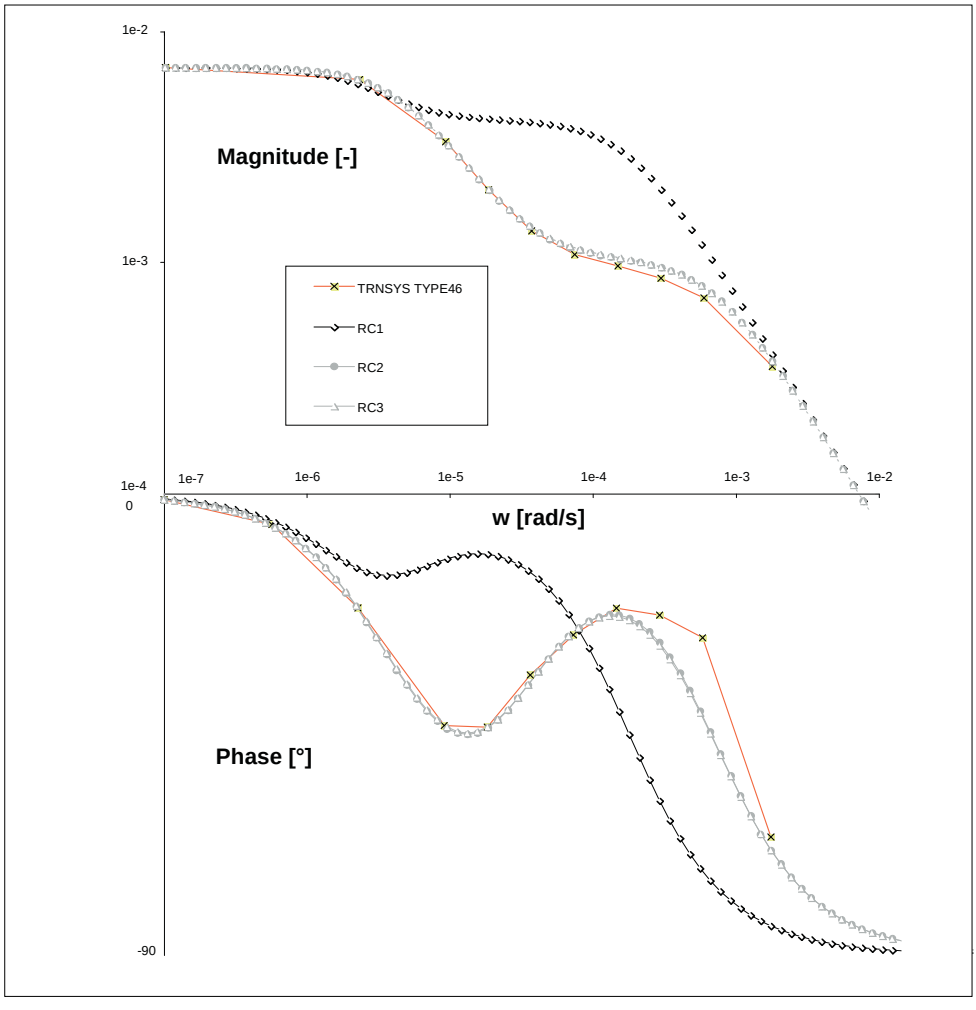

Figure 3: Bode's curve for testcell, convective heating

surprising considering the good performances of walls models for heat transmittance. On the other hand, heating and solar radiation are more difficult to deal excitations because heat fluxes are directly introduced on inside surface nodes, without thermal capacity. However, RC2 and RC3 give small errors, which shows that the assembly of walls and their connection to an air node lessen the problems due to the absence of surface capacity. The improvement:from RC1 to RC2 is very important, while RC3 gives roughly the same results as RC2.

The study of Bode's curves for the same excitations confirms these results. Figure 3 shows the frequency response to convective heating. RC2 and RC3 give an excellent response up to high frequencies (the highest frequency applied to the TYPE 46 corresponds to a 1h period). On the other hand, the RC1 model gives important errors even at moderate frequencies. Mag-nitude error is significant for periods ranging from 2 hours to 8 days, and so is the phase error for frequencies shorter than 15 days. This model is not only unable to cope with high frequency disturbances coming from HVAC system or from solar gains, but also unable to follow a daily cycle. These conclusions are drawn from our simulation example which is rather severe, but they show that the RC1 model is unsuitable for passive solar buildings.

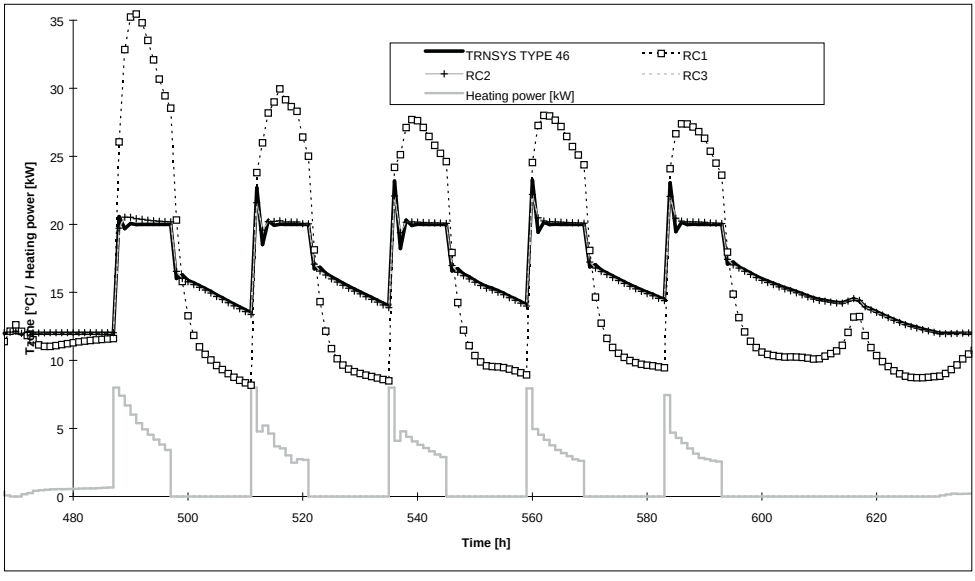

Figure 4 : TMY, fourth week of january

Table 2 : Testcell, error summary (TMY) [°C]						
Free-floating						
	RC1		**RC2**		**RC3**	
max(|ε|)	11.64	100 %	0.31	2.6 %	0.34	2.9 %
stddev(ε)	3.40	100 %	0.08	2.4 %	0.10	2.9 %
Heating(8000W max) & Cooling (4000 W max)						
	RC1		**RC2**		**RC3**	
max(|ε|)	19.62	100 %	1.21	6.2 %	1.27	6.5 %
stddev(ε)	5.02	100 %	0.21	4.2 %	0.22	4.5 %

The testcell simulation with real meteorological data is the last validation of our models before the comparison with experimental data which will be conducted for parameter identification. The fig 4 presents a selected week during the coldest period of the year, showing the maximum errors. The table 2 presents the error summary for the whole year, in the free-floating and in the heated/cooled case. All models present higher errors in the heated case, due to high frequency disturbances (e.g. when a heating step is applied at the start hour). The RC1 model presents a poor agreement with the TYPE 46 even in the free-floating situation, which confirms its non-suitability for our testcell.
RC2 has far better performances, while RC3 is not superior to RC2. Both present a good agreement with the TYPE 46, even with heating and cooling. The RC2 model's error stay below 1°C and has a standard deviation of 0.21°C, which makes it suitable for control. These performances are indeed excellent considering other error sources and the validity of the temperature uniformity hypothesis.

3. Application to optimal control

This section presents as an illustration an application of the linear state-space model described here above to the optimal control of our testcell. The aim is to assess the improvement due to the developed model, and not to study the control algorithm itself. We

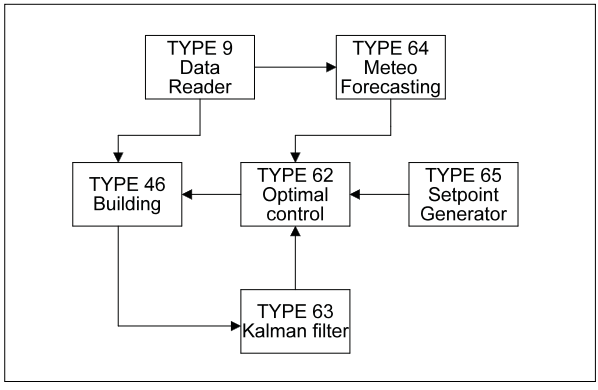

Figure 5: TRNSYS simulation scheme

used the TRNSYS environment to simulate the control system and the controlled building. The simulation scheme is presented fig. 5. The TYPE 46 is used to represent the testcell. The regulator consists in the Kalman filter (TYPE 63) and the optimal control algorithm itself (TYPE 62). Both routines use a simplified state-space model of the testcell. An additional routine that provides the meteorological forecasting should be included in a real application. The desired comfort temperature is given by the TYPE 65.

The used cost function which is minimised over a 24 h horizon is:

$$J = \sum_{k=1}^{24} \left[\alpha \left(T_{z,k} - T_z^s \right)^2 + \beta U_k^{\,2} \right]$$

where α and β are wheighting factors, T_z is the room temperature and T_z^s is the desired comfort temperature. The k subscript denotes the timestep (1 hour).
The optimal control sequence is computed each day at 00:00 and applied without any feedback compensation. Figure 6 shows the temperature profile for a typical heating day when the regulator:uses the RC1 and the RC2 models with the same wheighting factors. Note that the optimal temperature profiles are different because they depend on the model used by the algorithm. This explains that, with the same cost function's weighting factors, the optimal trajectory is closer to the comfort temperature for RC1. The "real" temperature, simulated here by the TYPE 46, does not follow exactly the desired trajectory because of model inaccuracies. However, the difference between the desired and the obtained

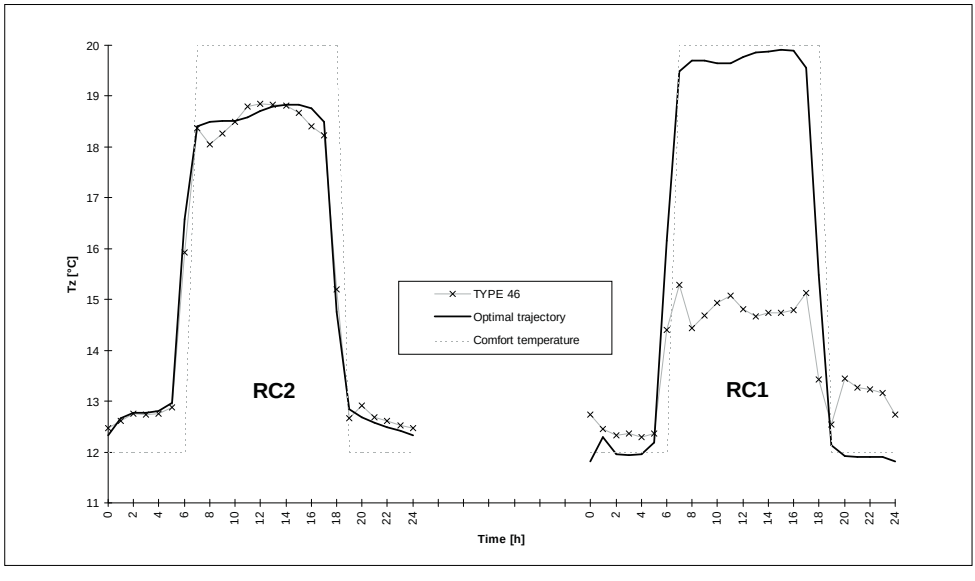

Figure 6 : simplified model comparison, intermittent heating

temperatures is drastically reduced by using the RC2 model. This does not cancel the need for a feedback compensation but it ensures that this correction will be as small as possible and will not compromise the optimal characteristic of the applied control sequence.

Conclusions

Homogeneous and multi-layer slabs can be modeled with a sufficient accuracy by a second-order lumped capacitance model. The step and frequency responses show an important improvement compared to the first order model. On the other hand, the addition of one node to obtain a third order model gives only a little improvement, and is not justified for our control application.

Thermal zone models obtained by the assembly of several second order slab models and one air node improve drastically the performances compared to the model obtained with first order slab models. Here again, the use of third order slab models does not seem to be justified, keeping other error sources in mind. The performances of the studied RC2 model make it suitable for control and are very good keeping other error sources in mind.

The experimental validation of the developed model is necessary and will be realised during the study of identification methods, with experimental data from the FUL's passive solar building.

References

[0] Kummert (M.), André (Ph.) et Nicolas (J.) - Modèles simplifiés de parois et de zones thermiques pour la commande optimale de bâtiments solaires. Paper submitted to the Revue Générale de Thermique.

[1] Winn (R.C.) and Winn (C.B.) - Optimal control for auxiliary heating of passive-solar-heated buildings. Solar Energy, 1985, vol. 35, n°5, p. 419-427.

[2] Rosset (M.M.) et Benard (C.) - Optimisation de la conduite du chauffage d'appoint d'un habitat solaire à gain direct. Revue Générale de Thermique, 1986, vol. 291, p. 145-159.

[3] Zaheer-Udin (M.) - Optimal control of a single-zone environmental space. Building and Environment, 1992, vol. 27, n°1.

[4] Fulcheri (L.), Neirac (F.P.), Le Mouel (A.) et Fabron (C.) - Chauffage des bâtiments. Intermittence et lois de régulation en boucle ouverte. Revue Générale de Thermique, 1994, n°387, p. 181-189.

[5] André (Ph.), Nicolas (J.) - Application de la théorie des systèmes à la thermique du bâtiment. Problèmes de modélisation, d'identification, de contrôle. Revue Générale de Thermique, 1992, n°371, p. 600-615.

[6] University of Wisconsin-Madison - TRNSYS. A transient simulation program. TRNSYS 13.1 Reference manual. 1990.

[7] Boileau (E.), Benard (C.) et Guerrier (B.) - Comparaison de différentes approximations des fonctions de transfert d'une paroi thermique. Revue Générale de Thermique, 1983, n°257, p.391-404.

[8] Benard (C.) - Optimisation de la représentation réduite d'une paroi thermique. International Journal of Heat and Mass Transfer, 1986, vol. 29, n°4, p. 529-538.

[9] Laret (L.) - Contribution au développement de modèles mathématiques du comportement thermique transitoire de structures d'habitation. Thèse de doctorat en Sciences Appliquées, Université de Liège, Laboratoire de Physique du bâtiment, 1980.

[10] Cotton (L.) and Nusgens (P.) - Multizone Building Dynamic Simulator of ATIC (MBDSA). User's guide. ATIC (Association Technique de l'Industrie du Chauffage, de la ventilation et des branches connexes), Bruxelles, 1990.